PHYSICAL REVIEW B, VOLUME 65, 134445

Anisotropic exchange in $LiCuVO_4$ probed by ESR

H.-A. Krug von Nidda,[1] L. E. Svistov,[1,2] M. V. Eremin,[1,3] R. M. Eremina,[1,4] A. Loidl,[1] V. Kataev,[4,5] A. Validov,[4] A. Prokofiev,[6] and W. Aßmus[6]

[1]*Experimentalphysik V, Elektronische Korrelationen und Magnetismus, Institut für Physik, Universität Augsburg, D-86135 Augsburg, Germany*

[2]*A. V. Shubnikov Institute of Crystallography, RAS, 117333 Moscow, Russia*

[3]*Kazan State University, 420008 Kazan, Russia*

[4]*E. K. Zavoisky Physical-Technical Institute, 420029 Kazan, Russia*

[5]*II. Physikalisches Institut, Universität zu Köln, D-50937 Köln, Germany*

[6]*Physikalisches Institut, Johann-Wolfgang-Goethe-Universität, D-60054 Frankfurt, Germany*

(Received 24 October 2001; published 29 March 2002)

We investigated the paramagnetic resonance in single crystals of $LiCuVO_4$ with special attention to the angular variation of the absorption spectrum. To explain the large resonance linewidth of the order of 1 kOe, we analyzed the anisotropic exchange interaction in the chains of edge-sharing CuO_6 octahedra, taking into account the ring-exchange geometry of the nearest-neighbor coupling via two symmetric rectangular Cu-O bonds. The exchange parameters, which can be estimated from theoretical considerations, agree nicely with the parameters obtained from the angular dependence of the linewidth. The anisotropy of this magnetic ring exchange is found to be much larger than it is usually expected from conventional estimations which neglect the bonding geometry. Hence, the data yield the evidence that in copper oxides with edge-sharing structures the role of the orbital degrees of freedom is strongly enhanced. These findings establish $LiCuVO_4$ as one-dimensional compound at high temperatures.

DOI: 10.1103/PhysRevB.65.134445 PACS number(s): 76.30.Fc, 75.30.Et

I. INTRODUCTION

In recent years experimental and theoretical studies of low-dimensional quantum magnetism of transition-metal (TM) oxides have received much attention. In particular, the discovery of a spin-Peierls transition in the one-dimensional Heisenberg antiferromagnet $CuGeO_3$ by Hase *et al.*[1] in 1993 triggered an intensive search for such a ground state in TM oxides with spin $S=1/2$ ions such as Cu^{2+} or V^{4+}. In this contents a lot of interesting low-dimensional compounds was investigated. However, up to now, no second inorganic spin-Peierls system was found, whereas this singlet dimerization of spin pairs is often observed in organic chain compounds. Even in the spin-ladder system NaV_2O_5, which exhibits a comparable magnetic susceptibility such as $CuGeO_3$, the ground state turned out to be driven by charge order.[2] In spite of this failure, recent research has brought into light another important aspect of magnetism of one-dimensional $S=1/2$ chains made of TM ions. A closer look at the properties of magnetic interactions in a number of Cu-based oxides revealed a surprisingly strong deviation from isotropic Heisenberg magnetism, which at first glance is not expected at all due to the quenching of the orbital angular momentum of Cu^{2+} by the crystal field.[3–6] Indeed, the magnetic anisotropy due to the orbital degrees of freedom plays a minor role in the two-dimensional cuprates, such as the parent compound of the high-T_c superconductors La_2CuO_4. The important difference between two- and one-dimensional Cu oxides arises from the fact that in the former the exchange interaction is usually mediated via a single 180° Cu-O-Cu bond, whereas in the latter the coupling often proceeds via two symmetric almost rectangular Cu-O-Cu bonds. The leading isotropic superexchange interaction $\mathcal{H}_{\rm iso}=\Sigma J_{ij}^{\rm iso}\mathbf{S}_i\cdot\mathbf{S}_j$ is reduced very strongly when going from 180° to 90°, as it follows from the Goodenough-Kanamori-Anderson rules.[7] However, it turns out that this reduction does not concern the anisotropic corrections to $\mathcal{H}_{\rm iso}$. This is, for example, justified by the observation of a very large spin-wave gap in Li_2CuO_4,[3] a large size of the ordered moment in $Ca_2Y_2Cu_5O_{10}$,[4] or extremely anisotropic magnetic order and a very broad electron-spin-resonance (ESR) linewidth in the paramagnetic state of $La_5Ca_9Cu_{24}O_{41}$.[5,6] The subject of the present paper, $LiCuVO_4$, exhibits Cu chains comparable to $CuGeO_3$ and to the other Cu oxides mentioned above, but it has been discussed controversially as a one- or two-dimensional antiferromagnet.[8,9]

$LiCuVO_4$ crystallizes within an inverse spinel structure AB_2O_4, which is orthorhombically distorted due to the cooperative Jahn-Teller effect of the Cu^{2+} ions (electronic configuration $3d^9$). The nonmagnetic V^{5+} ions are placed on the A positions in oxygen tetrahedra, whereas Li^+ and Cu^{2+} occupy the B positions in oxygen octahedra.[10] Both LiO_6 and CuO_6 octahedra form independent chains along the a and b directions, respectively, which themselves built up a stack of independent planes of Li and Cu rods along the c direction.[11] The detailed crystallographic data and a picture of the structure of $LiCuVO_4$ are given by Lafontaine *et al.*[12] The chains consist of edge-sharing octahedra with two nearly rectangular Cu-O-Cu superexchange bonds between every two Cu ions. Within the planes, neighboring chains are connected with each other by VO_4 tetrahedra forming Cu-O-V-O-Cu superexchange bonds. As from Goodenough-Kanamori-Anderson rules the 90° Cu-O-Cu superexchange is expected to be ferromagnetic, but becomes antiferromagnetic for slight deviations of the bond angle from 90° as well as due to possible side-group effects,[13] the relative strength of the different exchange paths is still unknown.

Due to this uncertainty, the magnetic susceptibility of $LiCuVO_4$ has been interpreted in different ways.[8–10,14] With decreasing temperature the susceptibility deviates from its high-temperature Curie-Weiss law $\chi \propto (T-\Theta_{CW})^{-1}$ with $\Theta_{CW} = -15$ K. It develops a first broad maximum close to $T_{max} = 28$ K, which is followed by a second sharper peak around 3 K, and finally drops down below $T_N = 2.3$ K. Originally the broad maximum was ascribed to two-dimensional antiferromagnetism between the Cu chains within one plane, and the sharp peak to the onset of three-dimensional order.[8,10] Later, one-dimensional antiferromagnetism has been proposed to explain the behavior around 28 K followed by two-dimensional correlations near 3 K (Ref. 9) and finally three-dimensional order at 2.3 K.[14]

Recently, ESR has been carried out in polycrystalline $LiCuVO_4$ by Vasil'ev *et al.*[15] The spectra reveal the typical pattern due to a uniaxial anisotropy of the resonance field, which allows one to determine the g values $g_\parallel$ and $g_\perp$ and the linewidths $\Delta H_\parallel$ and $\Delta H_\perp$ for the magnetic field applied parallel or perpendicular to the local symmetry axis, respectively. The g values, which are found to amount $g_\parallel = 2.25$ and $g_\perp = 2.08$ at high temperatures, are typical for Cu^{2+} in tetragonally distorted octahedral environment. As the long axis of the CuO_6 octahedra is oriented along the crystallographic c direction, $g_\parallel$ can be identified with g_c. Below 100 K the anisotropy $g_\parallel - g_\perp$ slowly increases up to a factor 2 at T_N compared to the value at room temperature. The linewidth is of the order of 1 kOe revealing an anisotropy as well with $\Delta H_\parallel / \Delta H_\perp \approx 1.5$. Its temperature dependence exhibits a minimum near 16 K and increases monotonously with negative curvature on increasing temperature. To lower temperatures the linewidth diverges on approaching the onset of magnetic order.

In a previous work[16] we independently performed ESR experiments on oriented powder samples, where the single crystalline grains were aligned by a magnetic field along their c axis. The ESR spectra consist of a single Lorentzian line showing an orientation dependence in accordance to the results obtained by Vasil'ev *et al.* in randomly distributed powder. The integrated intensity of the ESR line was found in good agreement with the static susceptibility. Concerning the resonance linewidth, we discussed the strength and the possible type of anisotropy of the spin-spin coupling in $LiCuVO_4$. We estimated the contributions of dipole-dipole (DD), anisotropic exchange (AE), and Dzyaloshinsky-Moriya (DM) interaction to ΔH following the work of Yamada *et al.* in $CuGeO_3$,[17] which exhibits a comparable linewidth. From this estimation, only the DM interaction, which is of first order in the spin-orbit coupling and thus brings the largest anisotropic correction to $\mathcal{H}_{iso}$, yielded the appropriate contribution to the line broadening, whereas the contributions from AE and DD interactions were found to be one and two orders of magnitude too small, respectively. However, considering the symmetry of the unit cell, the DM interaction should be zero, because every two DM vectors along the Cu chains cancel each other. In addition, a recent theoretical study of ESR in one-dimensional magnets with the DM interaction claims that its contribution to the linewidth should be in any case of the same level as that of the symmetric anisotropic term.[18]

In the present paper, we take the advantage of the measurements in single crystals of $LiCuVO_4$, which allows us to study the angular dependence of the ESR spectrum very accurately. In particular, the angular variation of the linewidth provides us with insight into the magnetic interactions in this compound. We reanalyze the anisotropic exchange within the Cu chains using the ideas, which were recently proposed to explain the width of the ESR signal in the Cu-O chains of the so-called telephone-number compound $La_{14-x}Ca_xCu_{24}O_{41}$.[6] The situation in that compound is quite similar to $LiCuVO_4$, as every two Cu ions in the chain are connected with each other by two oxygen ions, giving rise to a strongly anisotropic ring exchange, which is one order of magnitude larger than we estimated before. We show that in the high-temperature limit the linewidth can be mainly described in terms of this strong symmetric anisotropic exchange and can rule out the presence of the DM interaction. Our results emphasize that an adequate description of the magnetic properties of low-dimensional Cu oxides requires a detailed study of the anisotropic couplings which depend sensitively on a particular bonding geometry.

II. ANISOTROPIC EXCHANGE IN THE CU CHAINS

A. ESR linewidth and *g* factor

We consider a system of exchange-coupled spins $\mathbf{S}_i$ with an effective spin Hamiltonian given by

$$\mathcal{H}_{\rm eff} = \sum_{i>j} [J_{ij}^{\rm iso}(\mathbf{S}_i \cdot \mathbf{S}_j) + \mathbf{S}_i \cdot \mathbf{J}_{ij} \cdot \mathbf{S}_j] + \sum_i \mu_B \mathbf{H} \cdot \mathbf{g} \cdot \mathbf{S}_i, \quad (1)$$

where the scalar $J_{ij}^{\rm iso}$ denotes the isotropic exchange between two spins i and j, and the tensor $\mathbf{J}_{ij}$ is the anisotropic interaction due to symmetric exchange and dipole-dipole interaction. The last term describes the Zeeman splitting of the spin states in an external magnetic field $\mathbf{H}$ with gyromagnetic tensor $\mathbf{g}$ and Bohr magneton μ_B. In the case of $LiCuVO_4$ it is enough to take into account the interaction between neighboring Cu spins within the Cu-O chains ($i = j+1 \rightarrow J_{ij}^{\rm iso} \equiv J$), where all Cu places are equivalent.[19] In the crystallographic coordinate system, where the Cartesian coordinates (x,y,z) are chosen parallel to the (a,b,c) axes of the orthorhombic unit cell, both the g tensor with components $(g_a,\ g_b,\ g_c)$ and the tensor of the anisotropic interaction $(J_{xx},\ J_{yy},\ J_{zz})$ are diagonal.

Following Anderson and Weiss,[20] in the case of strong exchange narrowing the ESR linewidth ΔH (in Oe) is obtained from the second moment M_2 of $\mathcal{H}_{\rm eff}$ via the relation

$$\Delta H = \frac{\hbar}{g \mu_B \omega_{\rm ex}} M_2, \quad (2)$$

where $\omega_{\rm ex} \approx J/\hbar = |J_{xy,xy}|/\hbar$ is the so-called exchange frequency due to the super-exchange coupling of the ground states $|xy\rangle$ (see the next subsection) and

$$g=\sqrt{g_c^2\cos^2\theta+(g_a^2\cos^2\varphi+g_b^2\sin^2\varphi)\sin^2\theta} \tag{3}$$

is the usual expression for the g factor. Polar angle θ (with respect to c) and azimuth φ (with respect to a) give the orientation of the external field in the crystallographic system. In coordinates $\tilde{x},\tilde{y},\tilde{z}$, where the $\tilde{z}$ axis is defined by the direction of the applied magnetic field $\mathbf{H}$, the second moment M_2 due to anisotropic exchange is given by[21,22]

$$M_2=2\frac{S(S+1)}{3}\{f_1(2\tilde{J}_{zz}-\tilde{J}_{xx}-\tilde{J}_{yy})^2+f_2\times 10(\tilde{J}_{xz}^2+\tilde{J}_{yz}^2)+f_3[(\tilde{J}_{xx}-\tilde{J}_{yy})^2+4\tilde{J}_{xy}^2]\}. \tag{4}$$

The factor 2 appeared due to the summation over next neighbors. The symbols f_1, f_2, and f_3 denote the so called spectral-density functions, as introduced by Pilawa.[22] f_1 corresponds to the secular part, whereas f_2 and f_3 correspond to nonsecular parts. $\tilde{J}_{\alpha\beta}$ are anisotropy parameters in notations of Ref. 21. On transformation to the crystallographic coordinates (x,y,z), we obtain the angular dependence (see the Appendix).

Usually the resonance field of the paramagnetic resonance is obtained from the first moment of the spin Hamiltonian. In our case we find for $\mathbf{H}||c$:

$$\hbar\omega_c=g_c\mu_B H_{\mathrm{res}}\left\{1-\frac{\chi_c(T)}{g_c\mu_B}(2J_{zz}-J_{xx}-J_{yy})\right\}, \tag{5}$$

where $\chi_c(T)$ is the susceptibility per one copper site along the c axis. One gets the analogous expressions for $\mathbf{H}||a$ and $\mathbf{H}||b$ by changing $(x,y,z;c)$ into $(y,z,x;a)$ and $(z,x,y;b)$, respectively. For the case that one-dimensional short-range-order effects in the chain are important we find, following to the method described by Nagata and Tazuke:[23]

$$\hbar\omega_c=g_c\mu_B H\left\{1-\frac{N(T)}{|J|}(2J_{zz}-J_{xx}-J_{yy})\right\} \tag{6}$$

and analogous expressions for a and b direction. Here $N(T)$ is given by

$$N(T)=\frac{1}{10x}\left[\frac{2+ux}{1-u^2}-\frac{2}{3x}\right],$$

$$u=x+\coth\left(-\frac{1}{x}\right),$$

$$x=\frac{k_BT}{2|J|S(S+1)}.$$

We note that at the specified choice of anisotropy parameters (axial symmetry along the chain) our expressions convert to those which are listed by Nagata and Tazuke.

B. Estimation of the anisotropic exchange parameters

As it was described by many authors (see, for example, Refs. 24,25), the anisotropic exchange (AE) appears due to a virtual hopping process of an electron or hole between the ground-state orbital d_{xy} and the excited states $d_{x^2-y^2}$, d_{yz}, and d_{zx} in combination with spin-orbit coupling. Here the notation "xy" and "x^2-y^2" is interchanged with respect to the conventional usage, because we have chosen the coordinate system along the crystal axes, where the x and y axes are rotated by 45° with respect to the Cu-O bonds in the chains. For Cu^{2+} with the $3d^9$ electron configuration there is a single hole with $S=1/2$ in the ground state. In our case the most effective path for hopping is from the d_{xy} orbital of one Cu ion (j) via an oxygen p orbital to the excited $d_{x^2-y^2}$ state of the neighboring Cu ion (i), as it is explained in Fig. 1. The excited $d_{x^2-y^2}$ state is connected to the ground state d_{xy} of the same Cu ion (i) via spin-orbit coupling $\xi(\mathbf{S}_i\cdot\mathbf{L}_i)$. Here $\mathbf{S}_i$ and $\mathbf{L}_i$ denote the spin and orbital momentum of the Cu ion (i), respectively. There is only one matrix element $\langle x^2-y^2|L_z|xy\rangle=-2i$ of the L_z operator, which connects the $d_{x^2-y^2}$ and d_{xy} states. Therefore this process contributes to J_{zz} only, yielding the AE parameter

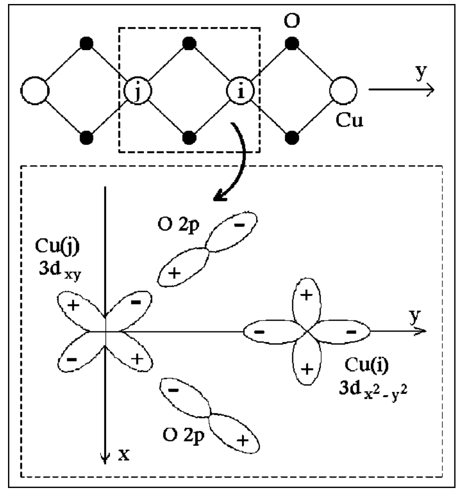

FIG. 1. Relevant orbitals to the strong anisotropy of the superexchange interaction between the Cu spins in the chain via a two-oxygen bridge. The coordinate y is chosen along the chain (b axis), z is perpendicular to Cu-O tape (c axis).

$$J_{zz}^{\mathrm{AE}}=2\left(\frac{\xi}{E_{x^2-y^2}-E_{xy}}\right)^2 J_{x^2-y^2,xy}=\frac{1}{32}(g_{zz}-2)^2 J_{x^2-y^2,xy} \tag{7}$$

with the energies E_{xy} and $E_{x^2-y^2}$ of the ground state and excited state, respectively. The AE parameters J_{xx}^{AE} and J_{yy}^{AE} are given by

$$J_{xx}^{\mathrm{AE}}=\frac{1}{2}\left(\frac{\xi}{E_{zx}-E_{xy}}\right)^2 J_{zx,xy}=\frac{1}{8}(g_{xx}-2)^2 J_{zx,xy}, \tag{8}$$

$$J_{yy}^{\mathrm{AE}}=\frac{1}{2}\left(\frac{\xi}{E_{yz}-E_{xy}}\right)^2 J_{yz,xy}=\frac{1}{8}(g_{yy}-2)^2 J_{yz,xy}. \tag{9}$$

Here $J_{\alpha,xy}$ (with $\alpha=x^2-y^2$, yz, zx) denotes the exchange-interaction parameter between one Cu ion in the ground state and the other Cu ion in the excited d_α state. In addition, we have to take into account the dipole-dipole (DD) interaction

$$J_{zz}^{\mathrm{DD}}=\mu_B^2\frac{g_{zz}^2}{R^3},\quad J_{xx}^{\mathrm{DD}}=\mu_B^2\frac{g_{xx}^2}{R^3},\quad J_{yy}^{\mathrm{DD}}=-2\mu_B^2\frac{g_{yy}^2}{R^3},\tag{10}$$

where R denotes the distance between neighboring Cu ions within the chains.

In the case under consideration, there are two bridging oxygen ions (see Fig. 1). As it was shown in Refs. 26,27, in such a geometry quantum interference between different exchange paths in the Cu-O plaquette strongly intensifies the ferromagnetic super-exchange coupling parameter $J_{x^2-y^2,xy}$ with respect to the parameter $J_{xy,xy}$ for the ground state of the copper ions. This was experimentally confirmed by ESR measurements of metal-organic complexes,[27] where an unusually large anisotropic exchange parameter J_{zz}^{AE} was found for Cu-Cu pairs connected via two bridging oxygen ligands. In the context of spin chains in copper oxides, such an effect was discussed in Refs. 28,29 as ring exchange.

In Ref. 27 the parameter $J_{x^2-y^2,xy}$ was estimated as -330 cm^{-1}. If we assume that this value is relevant for the case of $LiCuVO_4$ too, then with $g_{zz}-2=0.33$ (see Ref. 16 and the next section below), we expect $J_{zz}^{\mathrm{AE}}\approx-2$ K. The parameter $J_{zx,xy}$ has a ferromagnetic character (i.e., <0) and it is small with respect to $J_{x^2-y^2,xy}$, therefore J_{xx}^{AE} is not important. Using the Goodenough-Kanamori-Anderson rules, one can conclude that the parameter $|J_{yz,xy}|>|J_{zx,xy}|$. Unfortunately, it is not easy to estimate, but definitely J_{yy}^{AE} is not too small with respect to J_{yy}^{DD}. Substituting the intrachain Cu-Cu distance $R=2.786$ Å into the dipole-dipole terms, one should finally expect $J_{xx}\approx J_{xx}^{\mathrm{DD}}\approx0.12$ K, $J_{yy}\approx J_{yy}^{\mathrm{AE}}+J_{yy}^{\mathrm{DD}}\gg-0.24$ K, and $J_{zz}=J_{zz}^{\mathrm{AE}}+J_{zz}^{\mathrm{DD}}\approx-1.8$ K.

Using these results we can estimate the resonance linewidth in $LiCuVO_4$ from Eqs. (2) and (4). With the ground-state superexchange integral $J=J_{xy,xy}=-2\Theta_{\mathrm{CW}}=30$ K and the AE parameter J_{zz} estimated above, one obtains $\Delta H\approx1.5$ kOe. As we will see in the next section, this value is in very good agreement with the linewidth experimentally observed in single crystals of $LiCuVO_4$.

III. EXPERIMENTAL RESULTS AND DISCUSSION

The starting materials for synthesis of $LiCuVO_4$ were Li_2CO_3 (99.9%), V_2O_5 (99.5%), and CuO (99.5%). Single crystals of $LiCuVO_4$ were grown by slow cooling of a 40 mol. % solution of $LiCuVO_4$ in a $LiVO_3$ melt. The cooling from 675 to 580 °C was carried out with the rate of 0.8 °C/h. The details were described earlier.[30] X-ray diffraction analysis shows the absence of inclusions of other phases. The cell parameters derived from Rietveld refinement are $a=5.645$ Å, $b=5.800$ Å, and $c=8.747$ Å.

The ESR measurements were performed with a Bruker ELEXSYS E500 CW-spectrometer at X-band frequency ($\nu\approx9.35$ GHz), equipped with continuous gas-flow cryostats for He (Oxford Instruments) and N_2 (Bruker), which allow

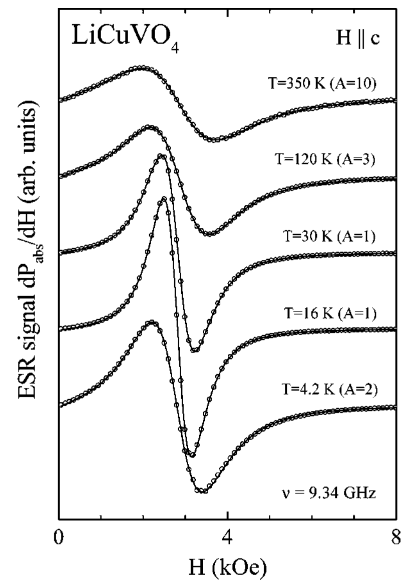

FIG. 2. ESR spectra of $LiCuVO_4$ for $\mathbf{H}||c$ at different temperatures. A denotes the relative amplification. The solid lines are fit curves due to Eq. (11).

us to cover a temperature range between 4.2 and 680 K. For temperatures down to 1.7 K, we used a cold-finger ^{4}He-bath cryostat. The ESR spectra record the power P_{abs} absorbed by the sample from the transverse magnetic microwave field as a function of the static magnetic field H. The signal-to-noise ratio of the spectra is improved by detecting the derivative dP_{abs}/dH with a lock-in technique. The $LiCuVO_4$ single crystals were glued on a suprasil-quartz rod, which allowed the rotation of the sample around defined crystallographic axes. The magnetic susceptibility was measured in a commercial superconducting quantum interference device (SQUID) magnetometer (Quantum Design) within a temperature range $1.8<T<400$ K.

In the paramagnetic regime, the ESR spectrum consists of a single exchange-narrowed resonance line[20] at all orientations of the magnetic field with respect to the crystallographic axes. Figure 2 illustrates typical ESR spectra for the magnetic field applied parallel to the c axis at different temperatures. The parameter A denotes the relative amplification factor. The resonance is well fitted by a Lorentzian line shape with a small contribution $|\alpha|\ll1$ of dispersion

$$\frac{dP_{\mathrm{abs}}}{dH}\propto\frac{d}{dH}\left[\frac{\Delta H+\alpha(H-H_{\mathrm{res}})}{(H-H_{\mathrm{res}})^2+\Delta H^2}+\frac{\Delta H+\alpha(H+H_{\mathrm{res}})}{(H+H_{\mathrm{res}})^2+\Delta H^2}\right].\tag{11}$$

As the linewidth ΔH is of the same order of magnitude as the resonance field H_{res} in the present compounds, Eq. (11) takes into account both circular components of the exciting linearly polarized microwave field and therefore includes the resonance at reversed magnetic field $-H_{\mathrm{res}}$.

Admixture of dispersion to the absorption signal is usually observed in metals, where the skin effect drives electric and magnetic microwave components out of phase in the sample.[31] Here, we are dealing with an insulator, where the asymmetry arises from the influence of nondiagonal ele-

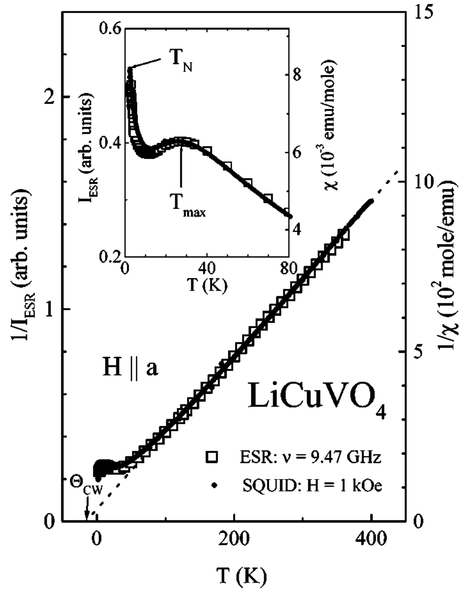

FIG. 3. Temperature dependence of the inverse ESR intensity $1/I_{\mathrm{ESR}}$ (left ordinate) and inverse static susceptibility $1/\chi$ (right ordinate) obtained by SQUID measurements. In both cases the magnetic field H has been applied parallel to the crystallographic a axis. The dotted line indicates a Curie-Weiss law with a Curie-Weiss temperature $\Theta_{\mathrm{CW}}=-15$ K. Inset: ESR Intensity (left ordinate) and static susceptibility (right ordinate) below 80 K with $T_{\max}\approx 28$ K and $T_N\approx 2.3$ K.

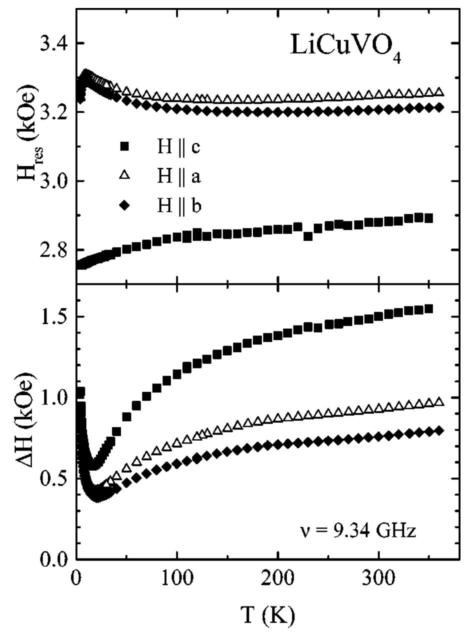

FIG. 4. Temperature dependence of resonance field (upper frame) and linewidth (lower frame) for the magnetic field applied parallel to the three crystallographic axes.

ments of the dynamic susceptibility: This effect is often observed in systems with interactions of low symmetry and sufficiently broad resonance lines ($H_{\mathrm{res}}\approx\Delta H$).[32]

The intensity I_{ESR} of the ESR line was determined from $I_{\mathrm{ESR}}=A_{\mathrm{sig}}\cdot\Delta H^2(1+\alpha)^{0.5}$, where A_{sig} denotes the amplitude of the ESR Signal dP_{abs}/dH. The ESR intensity measures the spin susceptibility and follows nicely the static susceptibility χ obtained by SQUID measurements, as it is shown in Fig. 3. The susceptibility is in well agreement with previous experiments,[8–10,14] which have been quoted in the Introduction. Now, even the slight discrepancy in the Curie-Weiss temperatures Θ_{CW}, which was found in powder samples between ESR and SQUID measurements,[16] can be ruled out as an artifact. The high-temperature Curie-Weiss law of both data extrapolates to $\Theta_{\mathrm{CW}}=-15$ K.

Figure 4 depicts the temperature dependence of resonance field and linewidth for the magnetic field applied parallel to all three crystallographic axes. We confined our measurements to temperatures below 400 K, because we found an irreversible increase of the resonance linewidth on heating to higher temperatures. Probably the heating in N_2 atmosphere reduces the oxygen content in the sample. The data are in good agreement with those obtained in polycrystalline samples.[16] In addition the single-crystal measurements reveal also an anisotropy in the ab plane. The ratio of the linewidth at high temperature amounts to $\Delta H_c:\Delta H_a:\Delta H_b=2:(5/4):1$. Below 200 K the temperature dependence of the linewidth is strongly nonlinear, whereas above 200 K it increases linear with temperature. The linewidth due to pure spin-spin relaxation always reaches an asymptotic value $\Delta H(\infty)$ at high temperatures. Assuming the linear behavior above 200 K due to additional relaxation processes via the lattice, we can treat the data at 200 K approximately as the asymptotic high-temperature value.

Figure 5 shows the full angular dependence of the resonance linewidth for the three crystallographic planes ab, ac, and bc at 200 K. The solid lines were obtained by the fit with Eq. (2) using the second moment of anisotropic exchange from Eq. (4).[33] The fitting parameters $J_{xx}=0.16$ K, $J_{yy}=-0.02$ K, and $J_{zz}=-1.75$ K agree nicely with the preliminary theoretical estimation in Sec. II.[34] It turns out that the AE parameter J_{zz} is indeed the dominant contribution, whereas J_{xx} can be understood in terms of DD interaction, alone. Concerning the parameter J_{yy}, which was difficult to estimate, the experiment indicates that both DD and AE

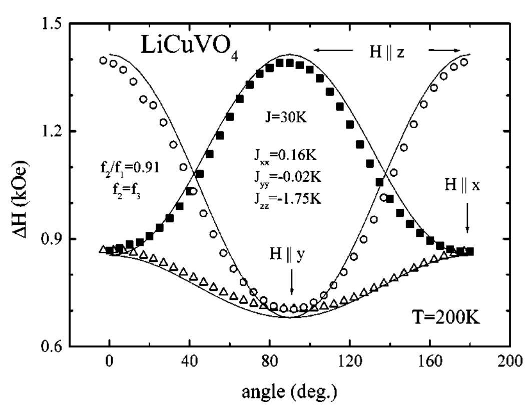

FIG. 5. Angular dependence of the resonance linewidth for three crystallographic planes. The x, y, and z direction have been chosen parallel to a, b, and c axis, respectively. The solid lines have been obtained from the fit as described in the text.

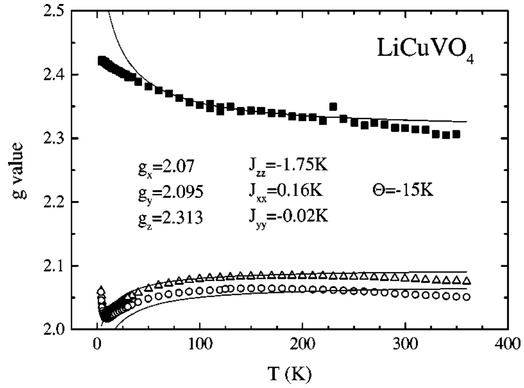

FIG. 6. Temperature dependence of the *g* value for the magnetic field applied parallel to the three crystallographic axes. The solid lines are fit curves as indicated in the text. The *x*, *y*, and *z* direction have been chosen parallel to *a*, *b*, and *c* axis, respectively.

nearly cancel each other. Remarkably, the largest anisotropic contribution to the superexchange amounts to about 6% of the leading isotropic coupling $J\approx 30$ K. Hence, it is three times larger than a conventional estimate of the anisotropy $\Delta J\sim(\Delta g/g)^2 J$, where Δg denotes the shift of the g factor from the spin-only value.[35] In terms of the linewidth the latter estimate yields a value, which is an order of magnitude smaller compared to the experimentally observed one.[16] That comparison of the theoretical predictions with the experimental data underlines the importance of the particular bonding geometry for the magnetic anisotropy of low-dimensional TM oxides.[36]

With the above estimates of the anisotropic exchange parameters the appropriate components of the g tensor $g_a=2.070$, $g_b=2.095$, and $g_c=2.313$ were obtained from the simultaneous fit of Eq. (5) to the temperature dependence of the g values, which is shown in Fig. 6. Using the Curie-Weiss susceptibility with $\Theta_{CW}=-15$ K, the fit curves reasonably reproduce the experimental data down to 25 K. The weak linear decrease of the g values with increasing temperature, which seems to be superposed, may arise from the slight change of the contribution α of dispersion with increasing linewidth (about 10% within the whole temperature range), which itself affects the resonance field [see Eq. (11)]. At lower temperatures ($T<25$ K), the experimental susceptibility is reduced with respect to the Curie-Weiss law, and therefore the data do not follow the divergence of the theoretical curve. We also tried to fit the g values with Eq. (6), which should better account for one-dimensional fluctuations, but this demands an even stronger divergence, which is not observed experimentally at all. This indicates the importance of the interchain couplings for the analysis of the low-temperature behavior.

For a complete analysis of the temperature dependence of the linewidth further theoretical effort is necessary. Not only the second moment but also the exchange frequency usually changes with temperature. Moreover, the interchain couplings have to be taken into account, as well.

IV. CONCLUSION

To summarize, we presented angular dependent ESR measurements in single crystals of $LiCuVO_4$. The anisotropic exchange interaction within the Cu chains was shown to account for the large linewidth and was successfully applied to describe its angular dependence. The anisotropic exchange parameters obtained from the experimental data well agree with theoretical estimations both in sign and magnitude. Hence from an ESR point of view, $LiCuVO_4$ turns out to be one dimensional at high temperatures. Notably the large magnetic anisotropy in the spin chains of this compound can be entirely described in terms of the anisotropic symmetric exchange only, without invoking the Dzyaloshinsky-Moriya interaction. Its relatively high value is due to a significantly enhanced role of the orbital degrees of freedom in the Cu-O chains with 90° bonding geometry. In this respect the present results may be important for the controversial discussion about the existence of the Dzyaloshinsky-Moriya interaction in $CuGeO_3$,[17,18,22,37] as well as for the better understanding of the magnetic properties of other low-dimensional transition-metal oxides.[38]

ACKNOWLEDGMENTS

We are grateful to D. Vieweg, M. Müller, and A. Pimenova for susceptibility measurements. We thank B. I. Kochelaev (Kazan-State University) for useful discussions. This work was supported by the Bundesministerium für Bildung und Forschung (BMBF) under Contract No. 13N6917 (EKM) and partly by the Deutsche Forschungsgemeinschaft (DFG) via the Sonderforschungsbereich (SFB) 484 and DFG Project No. 436-RUS 113/628/0. The work of M. V. Eremin was partially supported by University of Russia Grant No. N991327. The work of V. Kataev was supported by the DFG via Grant No. SFB 608, and that of A. Validov by the Russian Foundation for Basic Research RFBR (Grant No. N01-02-17533).

APPENDIX

On transformation of the anisotropic exchange parameters $\tilde{J}_{ij}$ to the crystallographic coordinates (x,y,z), we obtain in Eq. (4):

$$[2\tilde{J}_{zz}-\tilde{J}_{xx}-\tilde{J}_{yy}]^2=[J_{zz}(3\cos^2\beta-1)+J_{xx}(3\sin^2\beta\cos^2\alpha-1)+J_{yy}(3\sin^2\beta\sin^2\alpha-1)]^2,$$

$$\tilde{J}_{xz}^2+\tilde{J}_{yz}^2=[(J_{xx}\cos^2\alpha+J_{yy}\sin^2\alpha-J_{zz})\times\cos\beta\sin\beta+2J_{yz}\cos 2\beta\sin\alpha]^2+[(J_{yy}-J_{xx})\sin\beta\cos\alpha\sin\alpha]^2,$$

$$[(\tilde{J}_{xx}-\tilde{J}_{yy})^2+4\tilde{J}_{xy}^2]=[J_{xx}(\cos^2\beta\cos^2\alpha-\sin^2\alpha)+J_{yy}(\cos^2\beta\sin^2\alpha-\cos^2\alpha)+J_{zz}\sin^2\beta]^2+(J_{yy}-J_{xx})^2\times\cos^2\beta\sin^2 2\alpha.$$

Here we have taken into account that the g factor is anisotropic in our case and therefore

$$\cos\alpha = \frac{A}{\sqrt{A^2+B^2}}, \quad \cos\beta = \frac{C}{\sqrt{A^2+B^2+C^2}},$$

where

$$A = g_{xx}\sin\theta\cos\varphi, \quad B = g_{yy}\sin\theta\sin\varphi, \quad C = g_{zz}\cos\theta.$$

[1] M. Hase, I. Terasaki, and K. Uchinokura, Phys. Rev. Lett. **70**, 3651 (1993).

[2] P. Thalmeier and P. Fulde, Europhys. Lett. **44**, 242 (1998).

[3] M. Boehm, S. Coad, B. Roessli, A. Zheludev, M. Zolliker, P. Böni, D. McK. Paul, H. Eisaki, N. Motoyama, and S. Uchida Europhys. Lett. **43**, 77 (1998).

[4] H. F. Fong, B. Keimer, J. W. Lynn, A. Hayashi, and R. J. Cava, Phys. Rev. B **59**, 6873 (1999).

[5] U. Ammerahl, B. Büchner, C. Kerpen, R. Gross, and A. Revcolevschi, Phys. Rev. B **62**, R3592 (2000).

[6] V. Kataev, K.-Y. Choi, M. Grüninger, U. Ammerahl, B. Büchner, A. Freimuth, and A. Revcolevschi, Phys. Rev. Lett. **86**, 2882 (2001).

[7] J. B. Goodenough, Phys. Rev. **100**, 564 (1955); J. Kanamori, J. Phys. Chem. Solids **10**, 87 (1959); P. W. Anderson, Solid State Phys. **14**, 99 (1963).

[8] C. Gonzalez, M. Gaitan, M. L. Lopez, M. L. Veiga, R. Saez-Puche, and C. Pico, J. Mater. Sci. **29**, 3458 (1994).

[9] M. Yamaguchi, T. Furuta, and M. Ishikawa, J. Phys. Soc. Jpn. **65**, 2998 (1996).

[10] G. Blasse, J. Phys. Chem. Solids **27**, 612 (1965).

[11] M. O'Keefe and S. Andersson, Acta Crystallogr., Sect. A: Cryst. Phys., Diffr., Theor. Gen. Crystallogr. **33**, 914 (1977).

[12] M. A. Lafontaine, M. Leblanc, and G. Ferey, Acta Crystallogr., Sect. C: Cryst. Struct. Commun. **45**, 1205 (1989).

[13] W. Geertsma and D. Khomskii, Phys. Rev. B **54**, 3011 (1996).

[14] A. N. Vasil'ev, JETP Lett. **69**, 876 (1999).

[15] A. N. Vasil'ev, L. A. Ponomarenko, H. Manaka, I. Yamada, M. Isobe, and Y. Ueda, Phys. Rev. B **64**, 024419 (2001).

[16] Ch. Kegler, N. Büttgen, H.-A. Krug von Nidda, A. Krimmel, L. Svistov, B. I. Kochelaev, A. Loidl, A. Prokofiev, and W. Aßmus, Eur. Phys. J. B **22**, 321 (2001).

[17] I. Yamada, M. Nishi, and J. Akimitsu, J. Phys.: Condens. Matter **8**, 2625 (1996).

[18] J. Choukroun, J.-L. Richard, and A. Stepanov, Phys. Rev. Lett. **87**, 127207 (2001).

[19] We neglect the next-nearest neighbor (NNN) exchange interaction for the sake of simplicity, since it does not affect the conclusions of our qualitative discussion. In principal, it may be noticeable in $LiCuVO_4$ as in $CuGeO_3$. At least, the microscopic calculations in Ref. 29 suggest that, in general, the NNN exchange in the edge sharing Cu-O chain may be appreciable.

[20] P. W. Anderson and P. R. Weiss, Rev. Mod. Phys. **25**, 269 (1953).

[21] Z. G. Soos, K. T. McGregor, T. T. P. Cheung, and A. J. Silverstein, Phys. Rev. B **16**, 3036 (1977).

[22] B. Pilawa, J. Phys.: Condens. Matter **9**, 3779 (1997).

[23] K. Nagata and Y Tazuke, J. Phys. Soc. Jpn. **32**, 337 (1972).

[24] B. Bleaney and K. D. Bowers, Proc. R. Soc. London, Ser. A **214**, 451 (1952).

[25] K. Yosida, *Theory of Magnetism* (Springer, Berlin, 1996).

[26] M. V. Eremin and Yu. V. Rakitin, J. Phys. C **15**, L258 (1982).

[27] V. K. Voronkova, M. V. Eremin, L. V. Mosina, and Yu. V. Yablokov, Mol. Phys. **50**, 379 (1983).

[28] V. Yushankhai and R. Hayn, Europhys. Lett. **47**, 116 (1999).

[29] S. Tornow, O. Entin-Wohlman, and A. Aharony, Phys. Rev. B **60**, 10 206 (1999).

[30] A. V. Prokofiev, D. Wichert, and W. Assmus, J. Cryst. Growth **229**, 345 (2000).

[31] S. E. Barnes, Adv. Phys. **30**, 801 (1981).

[32] H. Benner, M. Brodehl, H. Seitz, and J. Wiese, J. Phys. C **16**, 6011 (1983).

[33] It is important to note that the best fit to the data was achieved choosing the spectral functions $f_2/f_1 = f_3/f_1 = 0.91$, where $f_1 \equiv 1$. In this case the angular dependence contains not only terms $\propto \cos^2$, which would be the case only, if $f_1 = f_2 = f_3$ is fulfilled, but also a modulation $\propto \cos^4$. Hence, the nonsecular part is slightly suppressed with respect to the secular. Obviously this effect should be interesting for a thermodynamic description.

[34] As one can see from the theoretical expressions, we really have only two fitting parameters, because the isotropic part $J_{xx}+J_{yy}+J_{zz}$ does not contribute to linewidth and shift.

[35] T. Moriya, Phys. Rev. **120**, 91 (1960).

[36] In principle one could also expect an anisotropic Curie-Weiss temperature due to the estimated anisotropic exchange. However, 6% anisotropic contribution to the exchange is still too small to give a measurable effect. For $\Theta_{CW} = -15$ K this is approximately 1 K, which is smaller than the experimental error.

[37] M. Oshikawa and I. Affleck, cond-mat/0108424 (unpublished).

[38] In spite of a comparable anisotropy of g value and high-temperature linewidth, in $CuGeO_3$ the situation seems to be more difficult, as the isotropic antiferromagnetic intrachain exchange is about 4 times larger than in $LiCuVO_4$ indicating a substantial deviation from 90° Cu-O-Cu bonding geometry. As it was shown by Tornow *et al.* (Ref. 29), in this case the anisotropic correction to the superexchange is significantly reduced as compared to the rectangular bond. Due to this fact one may expect a weaker magnetic anisotropy in $CuGeO_3$. In addition, the next-nearest neighbor contribution is more important.